

TDHF fusion calculations for spherical+deformed systems

A.S. Umar and V.E. Oberacker

Department of Physics and Astronomy, Vanderbilt University, Nashville, Tennessee 37235, USA

(Dated: August 12, 2018)

We outline a formalism to carry out TDHF calculations of fusion cross sections for spherical + deformed nuclei. The procedure incorporates the dynamic alignment of the deformed nucleus into the calculation of the fusion cross section. The alignment results from multiple E2/E4 Coulomb excitation of the ground state rotational band. Implications for TDHF fusion calculations are discussed. TDHF calculations are done in an unrestricted three-dimensional geometry using modern Skyrme force parametrizations.

PACS numbers: 21.60.-n, 21.60.Jz

I. INTRODUCTION

Heavy-ion fusion reactions are a sensitive probe of the size and structure of atomic nuclei [1]. Recent experiments with radioactive ion beams allow for the study of heavy-ion fusion with exotic nuclei. For instance, enhanced fusion-evaporation cross sections have been observed with neutron-rich ^{132}Sn beams on ^{64}Ni [2]. The synthesis of superheavy nuclei in hot and cold fusion reactions [3, 4, 5, 6, 7] represents another experimental frontier.

In general, the fusion cross sections depend on the interaction potential and form factors in the vicinity of the Coulomb barrier. Furthermore, experiments on subbarrier fusion have demonstrated a strong dependence of the total fusion cross section on nuclear deformation [8]. The dependence on nuclear orientation has received particular attention for the formation of heavy and superheavy elements [9] and various entrance channel models have been developed to predict its role in enhancing or diminishing the probability for fusion [10, 11]. While this may be true for heavy systems, the orientation effects should influence the fusion process for light nuclei as well.

There are several theoretical methods for calculating heavy-ion fusion cross sections: a) barrier penetration models [12, 13, 14], b) coupled-channels calculations [15, 16, 17, 18], and c) microscopic many-body approaches such as the Time-Dependent Hartree-Fock (TDHF) method [19, 20, 21, 22].

In recent coupled-channels calculations of heavy-ion fusion reactions, one typically uses the “rotating frame approximation” [17, 18] which assumes that the orbital angular momentum L of relative motion is conserved; this approximation avoids the full angular momentum coupling and thus reduces the number of coupled channels considerably. One tends to use empirical interaction potentials which are mostly real and energy-independent (Woods-Saxon potential, proximity-type potentials, double-folding potential). An imaginary potential is unnecessary because one takes into account explicitly all channel couplings that affect fusion. Coupling potentials are usually obtained utilizing macroscopic nuclear structure models (e.g. rotational model or harmonic vibrator). The coupled-channel equations

are solved numerically with standard scattering boundary conditions at $r \rightarrow \infty$, and an incoming-wave boundary condition at some point $r = R_F$ inside the Coulomb barrier. The fusion cross section is obtained from the incoming flux at R_F .

Fusion in the TDHF collision process is achieved when the relative kinetic energy in the entrance channel is entirely converted into internal excitations of a single well defined compound nucleus. In the TDHF theory the dissipation of relative kinetic energy into internal excitations is due to the collisions of the nucleons with the “walls” of the self-consistent mean-field potential. TDHF studies demonstrate that the randomization of the single-particle motion occurs through repeated exchange of nucleons from one nucleus into the other. Consequently, the equilibration of excitations is very slow and it is sensitive to the details of the evolution of the shape of the composite system. If one of the nuclei is deformed, one needs to carry out TDHF fusion calculations on a 3-D lattice for different relative orientations of the nuclei as they approach each other on a Rutherford trajectory, and afterwards one has to perform a suitable average over all orientations. Depending on the incident energy and impact parameter, some relative orientations may contribute to fusion while others may not. In lowest-order approximation, one might assume that all relative orientations of the intrinsic axis system occur with equal probability. This is indeed a reasonable approximation for relatively light nuclei where Coulomb excitation is negligible. However, in heavier systems, the dynamical alignment of the deformed nucleus as a result of multiple E2 and E4 Coulomb excitation of the ground state rotational band may no longer be ignored and results in a definite preferential alignment of the deformed nucleus which must be taken into account when calculating the fusion cross section.

There are a very limited number of TDHF collision studies involving deformed nuclei, and almost all of these were done in an axial geometry using the “rotating frame approximation”, and thus could not address the orientation dependence of reaction cross sections. Recently, we have developed a new TDHF code which assumes no symmetries regarding both the collision geometry and the Skyrme effective interaction [23] and utilizes the modern

Skyrme force parametrizations, including the time-odd terms. The numerical calculations are performed on a large 3-D Cartesian lattice using the Basis Spline collocation method [21] for increased accuracy. In this work we shall use this code to study fusion cross sections in the collisions of spherical+deformed nuclei.

The theoretical formalism for calculating the fusion cross section is outlined in Section II. In Section III we present fusion calculations carried out using this approach. In Section IV a summary and outlook is provided.

II. TDHF WITH ALIGNMENT

The evaluation of the heavy-ion collision dynamics can be divided into two separate steps: a) A dynamical Coulomb alignment calculation to determine the probability that a given nuclear orientation occurs at the distance $r(t_0)$, where the TDHF run is initialized. The distance $r(t_0)$ is chosen such that the nuclei only interact via the Coulomb interaction. b) A TDHF calculation, starting at this finite internuclear distance $r(t_0)$, for a fixed initial orientation of the deformed nucleus.

A. Coulomb excitation

For a given incident energy E_{cm} and impact parameter b , we carry out a semiclassical Coulomb excitation calculation of the dominant ground state rotational band of the deformed nucleus (see Fig. 1). The Coulomb excitation calculation starts at very large internuclear distances (about 1500 fm) when both nuclei may be presumed to be in their respective ground states. We have provided the details of this formalism in the Appendix. Fig. 2 shows a representative result in medium-mass nuclei,

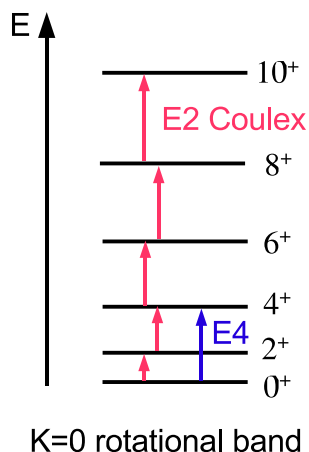


FIG. 1: Coulomb excitation of the ground state rotational band members via multiple E2 and E4 transitions.

For a given incident energy E_{cm} and impact parameter b , we carry out a semiclassical Coulomb excitation calculation of the dominant ground state rotational band of the deformed nucleus (see Fig. 1). The Coulomb excitation calculation starts at very large internuclear distances (about 1500 fm) when both nuclei may be presumed to be in their respective ground states. We have provided the details of this formalism in the Appendix. Fig. 2 shows a representative result in medium-mass nuclei,

as a function of time. In the Coulomb excitation code, we utilize the measured energy levels of the ground state rotational band in ^{162}Dy up to the 18^+ level [24]. We also use experimental values for the reduced transition probabilities [25] $B(E2, 0^+ \rightarrow 2^+) = 5.35e^2b^2$ and $B(E4, 0^+ \rightarrow 4^+) = 0.07e^2b^4$ from which one can calculate all remaining E2 and E4 matrix elements within the collective rotor model. In this semiclassical calculation, one can see how the nucleus “climbs up the rotational band” during the collision. Negative times in Fig. 2 correspond to the incoming branch of the Rutherford trajectory, and positive times correspond to the outgoing branch. The distance of closest approach is reached at $t = 0$. (Alternatively, one can plot the excitation probability as a function of the internuclear distance). The Coulomb excitation amplitudes, $a_{JM}(t)$, give rise to a preferential orientation (alignment). The dynamic alignment formalism presented in the Appendix allows us to follow the nuclear alignment as a function of the internuclear distance vector $\mathbf{r}(t)$. We would like to stress that the quantity which enters in our TDHF fusion calculations is not the Coulomb alignment after the reaction has taken place (at $t \rightarrow +\infty$) but rather the alignment at the *finite internuclear distance* $r(t_0) \approx 15\text{fm}$ on the incoming branch of the Rutherford trajectory. In the

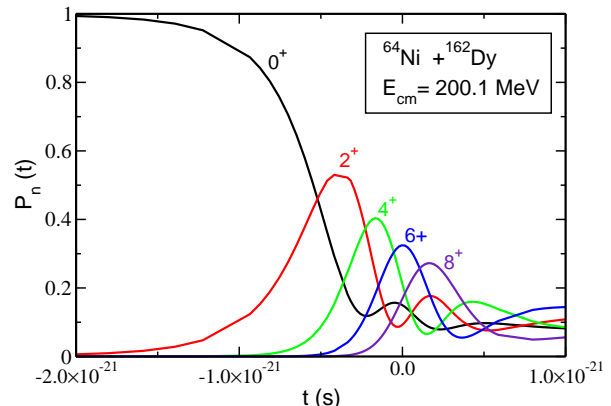


FIG. 2: Coulomb excitation probability of the $0^+, \dots, 8^+$ members of the ground state rotational band in ^{162}Dy as a function of time. The deformed nucleus is excited with a ^{64}Ni beam at $E_{cm} = 200.1 \text{ MeV}$ at impact parameter $b = 0$.

case of a spherical+deformed system, the relative orientation of the deformed nucleus may be specified by the three Euler angles (α, β, γ) relative to the collision plane as shown in Fig. 3. We use here the definition of the Euler angles given in Ref. [26]. Multiple Coulomb excitation predominantly excites the members of the $K = 0$ ground state rotational band which preserves an axially symmetric shape; hence, rotations about the symmetry axis z' described by the Euler angle γ are irrelevant (see Appendix).

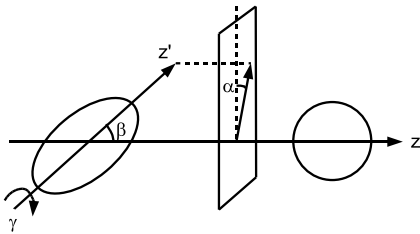


FIG. 3: The orientation of the intrinsic body-fixed frame of the deformed target nucleus is specified by the three Euler angles (α, β, γ) relative to the collision plane.

B. Fusion cross section

Subsequent to the determination of the initial conditions for the two nuclei, as described in the previous section, we perform a TDHF calculation to establish the outcome of the collision process. In TDHF, for a given set of initial conditions (energy, impact parameter, orientation, etc.), only one outcome is possible, thus we define

$$P_{TDHF}(b, E_{cm}; \beta, \alpha) = \begin{cases} 1 & \text{TDHF fusion} \\ 0 & \text{TDHF no fusion,} \end{cases} \quad (1)$$

where b is the asymptotic impact parameter, E_{cm} is the associated center of mass energy, and quantities β and α denote the orientation angles discussed above. The total fusion cross section may be written as

$$\sigma_{fusion}(E_{cm}) = 2\pi \int_0^{b_{max}} b db P_{fusion}(b, E_{cm}). \quad (2)$$

The probability for fusion is given in terms of the differential probability

$$P_{fusion}(b, E_{cm}) = \int d\Omega \frac{dP_{fusion}(b, E_{cm}; \beta, \alpha)}{d\Omega}, \quad (3)$$

where the Euler angle solid angle element is given by $d\Omega = \sin\beta d\beta d\alpha$, and

$$\frac{dP_{fusion}(b, E_{cm}; \beta, \alpha)}{d\Omega} = \frac{dP_{orient}(b, E_{cm}, t_0; \beta, \alpha)}{d\Omega} \times P_{TDHF}(b, E_{cm}; \beta, \alpha). \quad (4)$$

Since for a given E_{cm} value and angles (β, α) the TDHF fusion probability is either zero or unity we can instead write the integrals over the impact parameter to terminate at $b_{max}(\beta, \alpha)$, where $b_{max}(\beta, \alpha)$ denotes the maximum impact parameter for fusion for orientation angles β and α . This allows us to write

$$\frac{d\sigma_{fusion}(E_{cm}; \beta, \alpha)}{\sin\beta d\beta d\alpha} = 2\pi \int_0^{b_{max}(\beta, \alpha)} b db \times \frac{dP_{orient}(b, E_{cm}, t_0; \beta, \alpha)}{\sin\beta d\beta d\alpha}. \quad (5)$$

The differential cross section given in Eq. (5) in terms of Euler angles should not be confused with the laboratory differential cross section given in terms of the scattering angles. The differential orientation probability used in Eq. (5) is evaluated in the Appendix, Eq. (A.7).

III. NUMERICAL STUDIES

In order to gain a better insight into the differential orientation probability mentioned above we have performed calculations for systems that involve two heavy reaction partners and for systems which are composed of two light nuclei. We first examine the dynamical orientation, due to multiple E2/E4 Coulomb excitations, of the deformed nucleus $^{162}_{66}\text{Dy}$ colliding with a spherical $^{64}_{28}\text{Ni}$ nucleus at $E_{cm} = 265$ MeV. In a central collision (impact parameter $b = 0$), the orientation probability of an even-even nucleus is independent of the Euler angle α because, starting from the 0^+ ground state, only magnetic substates $M = 0$ of the ground state rotational band are excited. Therefore, the orientation probability depends only on the Euler angle β in this case (see Appendix, Eq. A.7). Fig. 4 shows the orientation probability for two values of the internuclear distance. At very large distance ($R = 1363$ fm) before the collision where the deformed nucleus is in its 0^+ ground state, all Euler angles β occur with equal probability, and there is no preferential alignment. However, at an internuclear distance of $R = R_1 + R_2 + 2 = 13.2$ fm (where R_1 and R_2 denote the mean square nuclear radii), we observe substantial alignment preference. Clearly, the perpendicular orientation ($\beta = 90^\circ$) is preferred over the parallel ($\beta = 0^\circ$) orientation, with an alignment ratio $dP(\beta = 90^\circ)/d\Omega / dP(\beta = 0^\circ)/d\Omega = 1.54$. The reason for this preferred alignment is easily understood in terms of classical electrostatics: for a given internuclear distance R , the perpendicular orientation of the deformed nucleus minimizes the Coulomb interaction energy which is proportional to $P_2(\cos\beta)$.

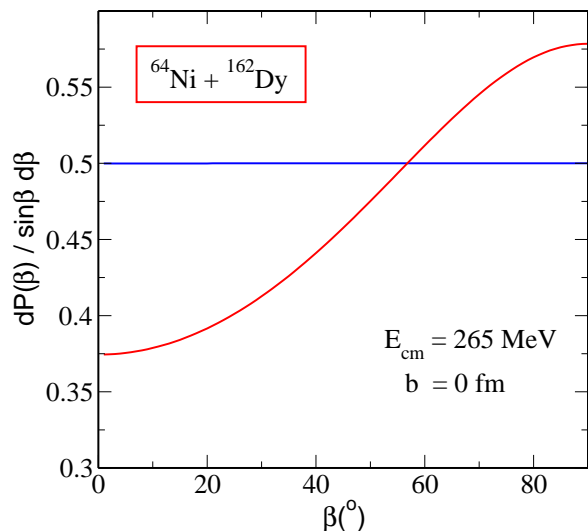


FIG. 4: Dynamic alignment due to Coulomb excitation of ^{162}Dy by a ^{64}Ni beam. Shown is the orientation probability as a function of the Euler angle β in a central collision at internuclear distances $R = 1363$ fm (blue curve) and at $R = 13.2$ fm (red curve).

We have repeated the above analysis to study the Coulomb excitation of the deformed nucleus ^{22}Ne in a central collision with an ^{16}O nucleus. In the Coulomb excitation code, we utilize the measured energy levels of the ^{22}Ne rotational band up to the $6^+(6.311\text{MeV})$ level [24]. The $B(E2, 0^+ \rightarrow 2^+)$ value is computed from the measured half-life [25] $T_{1/2} = 3.63\text{ps}$, and the remaining E2 matrix elements are determined from the collective rotor model. Fig. 5 shows the corresponding orienta-

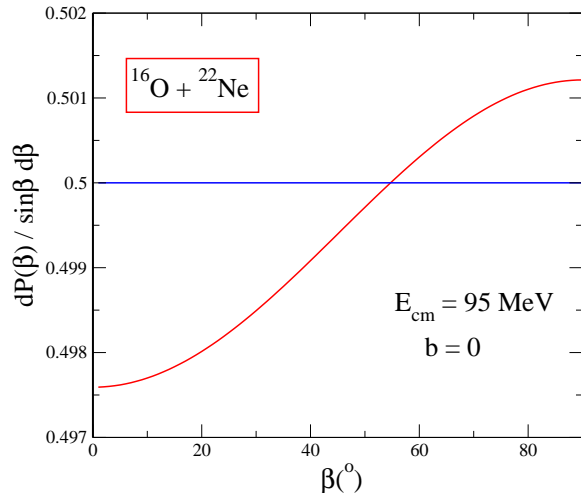


FIG. 5: Dynamic alignment due to Coulomb excitation of ^{22}Ne by a ^{16}O beam. Shown is the orientation probability as a function of the Euler angle β in a central collision at internuclear distances $R = 154$ fm (blue curve) and at $R = 14$ fm (red curve).

tion probability for these two light nuclei. Despite the much higher incident energy of $E_{cm} = 95$ MeV (about 6.9 times the Coulomb barrier height), we observe only a very small alignment preference: $dP(\beta = 90^\circ)/d\Omega / dP(\beta = 0^\circ)/d\Omega = 1.007$. There are two aspects pertaining to the importance of dynamical alignment in calculating fusion cross sections. In the case where all orientations lead to fusion the alignment probability provides a properly weighted sum for calculating the fusion cross section using Eq. (3). However, implicit in the above expression is also the fact that for different orientations we will have different values for b_{max} . Thus, even in a case where the central collision leads to fusion for all orientations of the deformed nucleus, and even if the Coulomb excitation probabilities are angle-independent, we still have different contributions to the fusion cross section arising from different orientations.

In order to demonstrate the points made above we have performed TDHF calculations for the $^{16}\text{O} + ^{22}\text{Ne}$ system at $E_{cm} = 95$ MeV. We have chosen this light system at a relatively high beam energy so that we can perform the numerical calculations faster. We have used our new TDHF code [23], which works in 3-D and uses modern Skyrme forces, including the time-odd terms. For this work we have used the SLy4 parametrization [27]. In

this case Hartree-Fock calculations result in a spherical ^{16}O nucleus and a ^{22}Ne nucleus with strong axial deformation. When no spatial symmetries are assumed Hartree-Fock calculations generate an orientation for the intrinsic coordinate system, with respect to the code coordinate system, typically determined by the choice for the initial single particle states, e.g. harmonic oscillators. Depending on the order in which the Cartesian oscillator shells are filled we get a particular orientation for the nucleus. Different orientations with Euler angle $\beta \neq 0$ can be generated by rotating the coordinate frame in which the initial single particle states are created with respect to the code frame. The resulting states will then be oriented with Euler angle β with respect to the code frame. A subsequent rotation perpendicular to this direction would then generate the α rotation. The Hartree-Fock iterations in generating the static solutions preserve this orientation since in an unrestricted geometry all orientations are exactly equivalent.

We have performed calculations by keeping the angle α fixed at $\alpha = 0^\circ$ and varying the angle β in 10° intervals. At this energy, all angles up to $\beta = 60^\circ$ do not show any fusion for head-on collisions, whereas larger angles fuse. For each of the orientations leading to fusion we have made a sweep over the impact parameter to find the maximum impact parameter for fusion. This was initially done in 1.0 fm steps and reduced down to 0.05 fm when the approximate fusion boundary was located. For large impact parameters the system undergoes multiple revolutions before fusion or deep-inelastic collision. Starting from an initial separation of 15 fm we have followed most of the collisions to about 1200 fm/c. Angles smaller than $\beta = 60^\circ$ contribute to the deep-inelastic channel. For these orientations a study of the central collisions show a gradual decrease in the translational kinetic energy between the two final fragments, ranging from almost 30 MeV for $\beta = 0^\circ$ to about 11 MeV for $\beta = 50^\circ$. We also observe particle transfer between the fragments, in most of the cases the final fragments seem to have exchanged one neutron from the Neon to the Oxygen. In the fusion regime we have found maximum impact parameters for fusion as 6.35 fm, 6.55 fm, 6.83 fm, and 6.87 fm for β values of 60° , 70° , 80° , and 90° , respectively. In Fig. 6 we show various time slices of the TDHF evolution for the case of $\beta = 60^\circ$ and $b = 6.35$ fm. During this time interval the system makes about four revolutions and eventually the internal structure shows no memory of the initial structure.

For Euler angles $\beta = 60^\circ$, 70° , 80° , and 90° , respectively, we find $^{16}\text{O} + ^{22}\text{Ne}$ fusion cross sections $d\sigma_{fusion}(E_{cm} = 95\text{MeV}; \beta, \alpha = 0^\circ)/\sin\beta d\beta d\alpha$ of 633 mb/sr, 673 mb/sr, 732 mb/sr, and 741 mb/sr.

IV. CONCLUSIONS

To date most TDHF calculations have been limited to the study of collisions involving spherical systems. Fur-

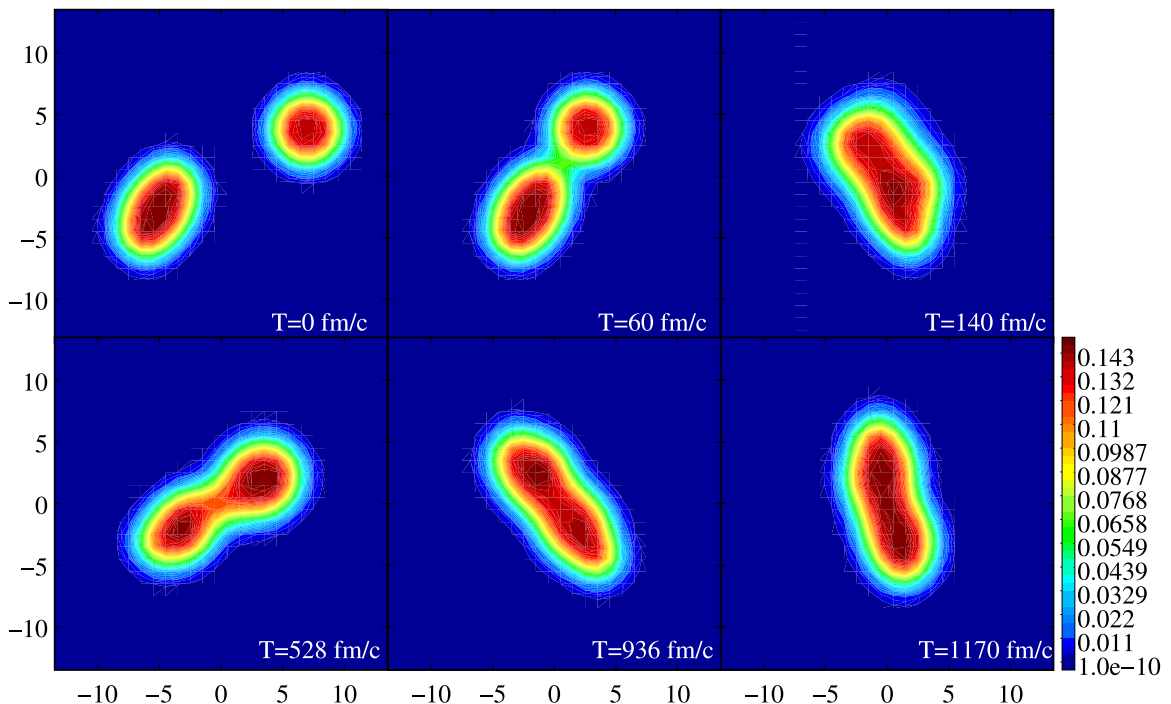


FIG. 6: TDHF time-evolution for the $^{22}\text{Ne} + ^{16}\text{O}$ collision at an impact parameter of $b = 6.35$ fm and initial Neon orientation angle $\beta = 60^\circ$ using the SLy4 interaction. The initial energy is $E_{cm} = 95$ MeV. During the evolution the combined system makes four revolutions.

thermore, approximations made about the collision geometry (reaction-plane symmetry etc.), in order to make numerical computations tractable, have led to the exclusion of deformed systems from such studies. In this paper, we have presented TDHF calculations involving spherical+deformed systems without any assumptions regarding collision geometry and using the full form of the Skyrme interaction. The details of our new TDHF code can be found in Ref. [23]. Dealing with deformed nuclei necessitates an approach to determine the orientation of the deformed system prior to the start of the TDHF calculations, as such calculations are initialized at relatively small separations. This alignment is inherently related to multiple E2/E4 excitations due to the Coulomb interaction between the two nuclei. We have outlined an approach for calculating this dynamical alignment probability and have shown how to incorporate it into the cross section calculations. While the alignment probabilities for various orientations do not vary substantially for light systems they show considerable preference for particular orientations of heavier systems. On the other hand, we have also shown that the alignment has a major consequence for TDHF calculations. We have observed that in the $^{22}\text{Ne} + ^{16}\text{O}$ system alignments close to the collision axis ($\beta < 60^\circ$) results in no fusion whereas perpendicular alignments lead to fusion. Furthermore, the alignment naturally affects the impact parameter dependence of fusion for different orientations. With the advent of computer technology and numerical methods

unrestricted TDHF calculations are becoming more and more feasible. It is our goal to pursue and improve such calculations in order to provide a tool for studying heavy-ion collisions with as few computational restrictions as possible.

Acknowledgments

This work has been supported by the U.S. Department of Energy under grant No. DE-FG02-96ER40963 with Vanderbilt University. Some of the numerical calculations were carried out at the IBM-RS/6000 SP supercomputer of the National Energy Research Scientific Computing Center which is supported by the Office of Science of the U.S. Department of Energy.

APPENDIX: DYNAMIC ALIGNMENT OF DEFORMED NUCLEI DUE TO COULOMB EXCITATION

We present a brief summary of the theory of dynamic alignment of deformed nuclei during a heavy-ion collision. The alignment results from multiple E2/E4 Coulomb excitation of the ground state rotational band. Details, including a discussion of strong nuclear interaction effects can be found in Ref. [28]. The associated formfactors for inelastic Coulomb excitation and strong nuclear excita-

tion (proximity potential) have been derived for collective rotations and surface vibrations in Ref. [29].

There exists an extensive literature on the ‘semiclassical’ theory of multiple Coulomb excitation of heavy ions [30]. In this approach, the excitation process is described quantum mechanically, and the relative motion of the nuclei is treated by classical mechanics. The total Hamiltonian consists of the free Hamiltonian of the target nucleus, $H_0(X)$, and of the coupling potential for inelastic Coulomb excitation, $V_C(X, \mathbf{r}(t))$. The latter depends on the intrinsic coordinates of the target (X) and on the classical relative trajectory $\mathbf{r}(t)$.

The Coulomb excitation process is determined by the time-dependent Schrödinger equation

$$[H_0(X) + V_C(X, \mathbf{r}(t))] \psi(X, t) = i\hbar \frac{\partial}{\partial t} \psi(X, t) . \quad (\text{A.1})$$

The eigenstates of the target nucleus are given by

$$H_0(X) \phi_r(X) = E_r \phi_r(X) . \quad (\text{A.2})$$

We expand the time-dependent wavefunction in terms of the stationary eigenstates ϕ_r of the unperturbed Hamiltonian H_0

$$\psi(X, t) = \sum_r a_r(t) \phi_r(X) e^{-iE_r t/\hbar} \quad (\text{A.3})$$

resulting in a system of linear coupled differential equations for the excitation amplitudes as a function of time

$$i\hbar \dot{a}_r(t) = \sum_s a_s(t) \langle \phi_r(X) | V_C(X, \mathbf{r}(t)) | \phi_s(X) \rangle$$

$$\times e^{i(E_r - E_s)t/\hbar} . \quad (\text{A.4})$$

This system of differential equations is solved numerically by a combination of the fourth-order Runge-Kutta method and the Adams-Bashforth-Moulton (predictor-corrector) algorithm [31]. For the classical relative motion $\mathbf{r}(t)$ we utilize the ‘coordinate system B’ defined in Ref. [30], page 47.

In the specific application of this formalism to dynamic nuclear alignment, we describe the free Hamiltonian and the corresponding wavefunctions in terms of the collective rotor model. The degrees of freedom are the three Euler angles $X = (\alpha, \beta, \gamma)$

$$H_0(X) = T_{rot}(X) . \quad (\text{A.5})$$

In deformed even-even nuclei, the ground state rotational band has an intrinsic total angular momentum projection $K = 0$; therefore, the collective rotor wavefunctions [26] are independent of the Euler angle γ which describes a rotation about the intrinsic symmetry axis z' (see Fig. 3)

$$\begin{aligned} \phi_r(X) &= \left(\frac{2J+1}{8\pi^2} \right)^{1/2} D_{M, K=0}^J(\alpha, \beta, \gamma) \\ &= (2\pi)^{-1/2} Y_{JM}(\beta, \alpha) . \end{aligned} \quad (\text{A.6})$$

The probability density at time t to find the nucleus oriented with given Euler angles $X = (\alpha, \beta)$ is given by $|\psi(X, t)|^2$; by integration over γ we find the corresponding differential orientation probability

$$\frac{dP_{orient}(b, E_{cm}, t; \beta, \alpha)}{\sin \beta d\beta d\alpha} = \int_0^{2\pi} d\gamma |\psi(\alpha, \beta, \gamma; t)|^2 \rightarrow \left| \sum_{J, M} a_{JM}(t) Y_{JM}(\beta, \alpha) e^{-iE_J t/\hbar} \right|^2 . \quad (\text{A.7})$$

-
- [1] R. Bass, *Nuclear Reactions with Heavy Ions*, (Springer-Verlag, New York, 1980).
- [2] J. F. Liang et al., Phys. Rev. Lett. **91**, 152701 (2003); Erratum: Phys. Rev. Lett. **96**, 029903 (2006).
- [3] S. Hofmann et al., Eur. Phys. J. A **14**, 147 (2002).
- [4] T. N. Ginter et al., Phys. Rev. C **67**, 064609 (2003).
- [5] Yu. Ts. Oganessian et al., Phys. Rev. C **69**, 021601(R) (2004).
- [6] K. Morita et al., Eur. Phys. J. A **21**, 257 (2004).
- [7] T. Ichikawa, A. Iwamoto, P. Möller, and A.J. Sierk, Phys. Rev. C **71**, 044608 (2005).
- [8] R. G. Stokstad, Y. Eisen, S. Kaplanis, D. Pelte, U. Smilansky, and I. Tserruya, Phys. Rev. Lett. **41**, 465 (1978).
- [9] K. Nishio, et al., J. Nucl. Radiochemical Sci., **3**, 89 (2002).
- [10] G. Fazio et al., Eur. Phys. J. A **19**, 89 (2004).
- [11] C. Simenel, Ph. Chomaz, and G. de France, Phys. Rev. Lett. **93**, 102701-1 (2004).
- [12] N. Takigawa and G.F. Bertsch, Phys. Rev. C **29**, 2358 (1984).
- [13] A. B. Balantekin and N. Takigawa, Rev. Mod. Phys. **70**, 77 (1998).
- [14] M. J. Rhoades-Brown and V. E. Oberacker, Phys. Rev. Lett. **50**, 1435 (1983).
- [15] S. Landowne and S. C. Pieper, Phys. Rev. C **29**, 1352 (1984).
- [16] M. J. Rhoades-Brown and M. Prakash, Phys. Rev. Lett. **53**, 333 (1984).
- [17] H. Esbensen, Prog. Theor. Phys. Suppl. **154**, 11 (2004).
- [18] K. Hagino, N. Rowley, and A.T. Kruppa, Comp. Phys.

- Comm. **123**, 143 (1999).
- [19] J. W. Negele, Rev. Mod. Phys. **54**, 913 (1982).
 - [20] P. Bonche, H. Flocard, P.-H. Heenen, S.J. Krieger, and M.S. Weiss, Nucl.Phys. **A443**, 39 (1985).
 - [21] A. S. Umar, M. R. Strayer, J.-S. Wu, D. J. Dean, and M. C. Güçlü, Phys. Rev. C **44**, 2512 (1991).
 - [22] A. S. Umar and V. E. Oberacker, Eur. Phys. J. A **25**, s01, 553 (2005).
 - [23] A. S. Umar and V. E. Oberacker, Phys. Rev. C (submitted); <http://arxiv.org/abs/nucl-th/0603038>.
 - [24] Evaluated Nuclear Structure Data File (ENSDF), National Nuclear Data Center, Brookhaven National Laboratory, <http://www.nndc.bnl.gov/ensdf/>.
 - [25] LBNL Isotopes Project, <http://ie.lbl.gov/toi.htm>.
 - [26] D. M. Brink and G.R. Satchler, *Angular Momentum*, 2nd ed., (Clarendon Press, Oxford, 1979).
 - [27] E. Chabanat, P. Bonche, P. Haensel, J. Meyer, and R. Schaeffer, Nucl. Phys. **A635**, 231 (1998); Nucl. Phys. **A643**, 441 (1998).
 - [28] V. E. Oberacker, Phys. Rev. C **32**, 1793 (1985).
 - [29] V. E. Oberacker, M. J. Rhoades-Brown, and G. R. Satchler, Phys. Rev. C **26**, 129 (1982).
 - [30] K. Alder and A. Winther, *Electromagnetic Excitation*, (North Holland, Amsterdam, 1975).
 - [31] W. H. Press, S. A. Teukolsky, W. T. Vetterling, and B. P. Flannery, *Numerical Recipes*, 2nd ed., (Cambridge University Press, Cambridge, 1992).